Available online at www.sciencedirect.com
ScienceDirect
Polymer 48 (2007) 1397–1409
polymer
www.elsevier.com/locate/polymer

Cavitation during tensile deformation of high-density polyethylene

Andrzej Pawlak*

Center of Molecular and Macromolecular Studies, Polish Academy of Sciences, Sienkiewicza 112, 90-363 Lodz, Poland

Received 25 October 2006; received in revised form 21 December 2006; accepted 31 December 2006
Available online 25 January 2007

Abstract

Cavitation process of high-density polyethylene during tensile deformation was studied. It has been shown that the crystallinity and perfection of HDPE crystals govern whether plastic deformation of the polymer is associated with cavitation or deformation occurs without cavitation. The strength of crystals may be controlled by crystallization conditions during preparation of a polymer. If the crystals are thin and the degree of crystallinity is low then the plastic deformation of crystals occurs before reaching the level of stress that initiates cavitation. On the other hand, if the crystals are thick, more perfect, and crystallinity is high, then the cavitation in an amorphous phase is initiated first, and later followed by the deformation of crystals. The cavitation process is usually initiated at the stress level close to the yield point. However, the level of stress necessary for cavitation may be decreased substantially by the orientation of crystalline lamellae, as it was observed in the skin layers of injection-molded material. Voids formed in the skin layer do not influence the yielding process. Typically, cavitation was initiated in volume at the stress of 29–30 MPa, but in the skin of injected samples voids were observed even at the macroscopic stresses of 2 MPa only. The development of voids with deformation was studied both for skin and volume of injection-molded HDPE sample. The shape of voids is strictly connected with deformation of crystalline phase around them.

Keywords: Cavitation; Plastic deformation; Polyethylene

1. Introduction

Cavitation during the deformation of crystalline polymers in tensile drawing was observed previously by many authors [1–7], however in other papers the phenomenon was treated as marginal, accompanying plastic deformation of polymer crystals. Butler et al. [3,6] studied plastic deformation of tensile drawn high-density polyethylene (HDPE) and detected an intensive cavitation by using small angle X-ray scattering (SAXS). Voids in polyethylene were formed at yield point, at the same moment when martensitic transformation and chain slips begins [6]. The increase in cavitation was observed during strain softening, i.e. decreasing of engineering stress after the yield. It was interpreted that the cavitation is initiated by releasing of constrains in polymer during lamellar disruption. In this paper and many others, even if the cavities were recognized the efforts of authors were concentrated on the mechanisms of plastic deformation in semi-crystalline polymers.

The mechanisms of plastic deformation are different for amorphous and crystalline phases. It is thought that the yield in crystalline polymers above their glass transition temperature is determined by the stress required for plastic deformation of crystals. The knowledge of plastic deformation of a crystalline phase is now rather well established, and such aspects as crystallographic slips, rearrangement of the lamellar structure, and the role of crystal defects were discussed in the literature [8–16]. The planes of an easiest slip and stresses of slip initiation, τ_0, were determined for some polymers. As an example the easiest slip for PA 6 is at $\tau_0 = 16.24$ MPa [17], but for polypropylene the observed (010)[001] slip is at $\tau_0 = 22$–25 MPa [12,18]. However, one must be aware that those measurements were conducted on highly textured materials in which the macromolecular chain entanglements from

* Tel.: +48 42 6803223; fax: +48 42 6847126.
E-mail address: apawlak@bilbo.cbmm.lodz.pl

0032-3861/$ - see front matter © 2007 Elsevier Ltd. All rights reserved.
doi:10.1016/j.polymer.2006.12.054

amorphous layers were incorporated into newly assembled crystals. Such systems may show lowered shear stress for crystallographic slip due to imperfection of crystals.

Only recently the cavitation has been recognized as an important factor that determines the way of plastic deformation of crystalline polymers in a microscale [8,19]. Pawlak and Galeski [19] showed that in many polymers, such as poly(methylene oxide) (POM), polypropylene (PP), or high-density polyethylene, intensive cavitation was observed in tensile drawing, leading to decrease of yield stress and yield strain. There is another group of polymers, such as low-density polyethylenes (LDPE) and other polymers with small crystals, in which cavities are not observed during tensile drawing. The differences in deformation behavior of those polymers were explained as a result of a competition between two processes: voiding in amorphous phase and plastic deformation of crystals. If the stress level for cavitation in the tensile test is lower than the stress of plastic deformation for lamellae, then intensive voiding between lamellae occurs, which has the influence on macroscopic yielding. This mechanism is visible in polymers with large crystals and high crystallinity, such as POM, PP or HDPE. If the crystals are small and defective, they deform plastically before reaching the stress necessary for cavitation of the amorphous phase in the sample. This was observed for LDPEs and other polymers.

The voids, if present, are located in amorphous layers between lamellae. The strength of an amorphous phase may be predicted by analogy from the observations of the cavitation in a crystallizing polymer melt. The values of negative pressure for cavitation for HDPE melt are scattered and are between −3.5 and −10 MPa [20]. It is known that if a surface tension is not compensated by local stress the small voids are unstable and quickly close [21]. Pawlak and Galeski [19] have shown that if the applied tensile stress is around 25 MPa, which was value of yield stress for analyzed HDPE, it is sufficient for initiation of cavitation and stabilization of bubbles with a radius of 5 nm and larger.

Usually the cavities are detected by visual observation of stress whitening or by small angle X-ray scattering [3,4,6]. G'Sell et al. [22,23] and Lazzeri et al. [24] applied the concept of volume strain [25] for the analysis of necking process and further plastic deformation of semi-crystalline polymers. It was shown that the measurement of volume change might be also a tool for detecting cavitation process [24].

There is controversy in the literature concerning measurement of the size of voids from SAXS patterns. One approach is based on the determination of Porod plots $s^4I(s)$ vs. s^4, where I is the scattered intensity and s is the scattering vector. Porod's constant K and invariant Q are used for the calculation of mean diameter of scattering objects [26,27]. The second way of size determination is an analysis of Guinier equation $\ln(I) = f(s^2)$ and calculation of radius of gyration (R_g). If the shape of cavities is known or assumed, the cavity mean dimension may be found from R_g [28,29].

The comparison of results of tensile and compression tests done by Pawlak and Galeski [19] lead to the conclusion that the presence of voids in deformed polymers depends on the yielding of crystal. If the yield stress is high, the cavitation is initiated, if not deformation of crystals without cavitation occurs. The yielding of crystals is related to their perfection and thickness, which in turn depends on crystallization conditions. One of the goals of this paper is to show that by changing the solidification conditions it is possible to switch from cavitational to non-cavitational deformation in the tensile drawing. A material suitable for such a study is compression molded high-density polyethylene (HDPE).

Injection-molded material is also of interest for the present study as some level of orientation is developed in a specimen. It is reasonable to expect that such orientation may influence the plastic deformation and initiation of the cavitation process.

2. Experimental

High-density polyethylene BASF Lupolene 6021D (M_w 1.8×10^5, $M_w/M_n = 7.2$, density 0.960 g/cm^3, MFI = 0.26 g/10 min at 2.16 kg, 190 °C) was selected for these studies. Samples for a mechanical test were prepared by an injection molding. A Battenfeld 30 g injection-molding machine was used. The temperature of a barrel was 185 °C and the temperature of mold was 20 °C. The shape of samples was according to ASTM D638M-93 standard, with 10 mm width and 4.0 mm thickness. The mold was with wide entrance and the speed of injection was low. Orientation effect in the injected polymer was reduced only to the thin surface layer.

A second batch of samples was prepared by a compression molding at the temperature of 190 °C, using a hot press. Three different procedures of cooling were applied: in the air (HDPE-A), in the water (HDPE-W) and in the water with ice (HDPE-WI). The 1, 2 and 4 mm thick sheets were produced. Dog-bone samples for mechanical tests were then cut from these sheets.

Mechanical tensile properties of HDPE were studied at room temperature using Instron model 5582 testing machine. Testing rate was 5%/min. The actual shape of a sample during deformation was recorded by a "Minolta Dimage" digital camera. A mirror was applied for simultaneous recording of the third dimension of a sample − the thickness. Actual cross-section was calculated from measured dimensions of the sample. For measurements of the local deformation, black marks were placed on the surface of the sample, at distances of 1 mm. The strain was determined as the change of distance between marks, $l - l_0$, divided by the original distance l_0. The volume strain was calculated as a change of volume, ΔV, divided by the initial volume, V_0, measured in the most deformed part of a sample.

The tensile drawing was stopped at a selected deformation level, and the stretched sample after fixing in a special frame was analyzed in the stressed state by small angle X-ray scattering.

The small angle X-ray scattering technique (SAXS) was used for detection of cavities and for determination of long periods. A 0.5 m long Kiessig-type camera was equipped with a pinhole collimator and a Kodak imaging plate as a recording medium. The camera was coupled to a Philips PW 1830 X-ray

generator (Cu Kα, operating at 50 kV and 35 mA) equipped with a capillary collimator, allowing for resolution of scattering objects up to 40 nm. Exposed imaging plates were read with a PhosphorImager SI system (Molecular Dynamics). The function of $\ln(I)$ vs. s^2, where I is intensity of scattering and s is scattering vector, was the base for calculation of radius of gyration (R_g). Details of the procedure are the same as described by Yamashita and Nabeshima [28]. Since the dependence $\ln(I) = f(s^2)$ was not linear for deformed HDPE it was divided into two to four, approximately linear parts, each of them representing another population of cavities. The contribution of each group of voids to the total scattering was determined and radii of gyration was then calculated, beginning with the smallest voids. However, the largest voids are not registered by SAXS apparatus because of its resolution which is below 40 nm.

The wide-angle X-ray scattering (WAXS) photo camera was used for observations of lamellae orientation. A source of Cu Kα radiation, operating at 50 kV and 35 mA was used. Two-dimensional scattered images were recorded by a camera equipped with a Kodak imaging plate. The distance between a sample and recording plate was 5 cm. Exposed imaging plates were analyzed with PhosphorImager SI system (Molecular Dynamics).

The degree of crystallinity, melting temperature and lamellar thickness were determined from the heat of melting and peak melting temperature by the use of a DSC 2920 differential scanning calorimeter (TA Instruments). The samples of weight 8–9 mg were heated in the range of temperature from 20 °C to 190 °C, at the rate of 10 K/min. The crystallinity was calculated from the area under the melting peak, assuming that the heat of fusion for HDPE is 280 J/cm^3 [30]. Properties of skin layers were determined for 0.3 mm thick slices cut parallel to the surface. The length of crystalline stem, l_c, was determined from the equation: $l_c = 2\sigma_e T_{mo}/(\Delta H_f \Delta T)$, where σ_e is lamellar basal surface free energy (for PE $\sigma_e = 9 \times 10^{-6}$ J/cm^2 [30]), T_{mo} is equilibrium melting temperature (418 K [31]), ΔH_f is heat of fusion per unit volume (for PE $\Delta H_f = 280$ J/cm^3), $\Delta T = T_{mo} - T$, T is melting temperature (position of maximum of DSC peak). The inclination of crystalline stems by 35° to the normal of lamellae surface [32] was taken into account in calculations of lamellae thickness L.

The crystallinity and lamellar dimensions were also analyzed by wide-angle X-ray scattering (WAXS). Computer controlled wide-angle goniometer coupled to a sealed-tube source of Cu Kα radiation, operating at 50 kV and 35 mA, was used. The Cu Kα line was filtered using electronic filtering and the usual thin Ni filter. 2θ scans were collected with a divergence angle of less than 0.05°. The Scherrer equation $L_{hkl} = 0.9\lambda/(\beta\cos\theta)$, where L_{hkl} is crystal size in the direction perpendicular to (hkl) plane, λ is wavelength, β is the half-width of diffraction peak, θ is the Bragg angle, was applied for determination of crystal sizes [33].

Samples for microscopic observations were prepared from a previously deformed material. A Tesla ultramicrotome equipped with a glass knife was used to remove 0.1 mm or 0.5 mm thick surface layers of the polymer. A revealed inner surface of the sample was then treated by a permanganic etchant in order to reveal lamellar structure. Specimens were etched according to the procedure developed originally by Olley and Basset [34] for 25 min in 2 wt% $KMnO_4$ solution in H_2SO_4/H_3PO_4 (1:1 vol). The etching process was quenched by immersing the specimen in cold diluted H_2SO_4. Then, the specimen was subsequently immersed into four tubes in an ultrasonic bath, containing the following liquids: diluted cold H_2SO_4, cold H_2O_2 (diluted, 30%), H_2O and acetone. Time of immersion in each tube was 3 min. The etched specimens were sputtered with gold and examined in a Jeol 5500 LV scanning electron microscope in a high vacuum mode.

3. Results and discussion

The initial structure of 1 mm thick compression-molded HDPE samples was characterized by DSC, WAXS and SAXS. Results of measurements of crystallinity degree and lamellae thickness are collected in Table 1. The data in Table 1 show that crystallinity and lamellae thickness depend on the cooling conditions during solidification. The thickest crystals (22.6 nm) measured by DSC and the highest crystallinity was observed for HDPE-A. This material was cooled in air, i.e. the temperature decreased slowly and the time of crystallization was the longest. With an increase of the cooling rate, the mean lamellae thickness decreased from 22.6 to 18.3 and 17.9 nm for HDPE-W and HDPE-WI, respectively. The degree of crystallinity in quickly cooled samples was lower by 11% than for HDPE-A.

The differences between values obtained from DSC and X-ray scattering experiments are small and the main tendency – the increase of crystal thickness and crystallinity with decreasing of cooling rate – is clear. The slightly larger values of lamellae thickness measured by DSC are probably the result of crystal thickening during heating of a polymer in DSC cell [35].

The shape of WAXS diffraction peaks may be an additional source of information about sizes of HDPE crystals. In the diffractograms of studied polyethylene only two strong reflections, representing (110) and (200) crystallographic planes, were seen. The most interesting dimension, crystal thickness, which influences yield process, is related to scattering from (002) plane. Unfortunately, the reflection from (002) plane was very weak and could not be used for calculation of thickness by Scherrer equation. However, it was possible to determine the undisturbed crystal dimension in the direction

Table 1
Characteristic of crystalline structure of compression molded, 1 mm thick samples

Sample	Crystallinity degree [%]		Crystalline stem length, l_c [nm]	Lamellae thickness, L [nm]	
	by DSC	by WAXS	by DSC	by DSC	by SAXS
HDPE-A	80	78	27.6	22.6	21.1
HDPE-W	69	70.5	22.4	18.3	13.9
HDPE-WI	69	68	21.8	17.9	13.2

perpendicular to (200) plane. The largest crystals in this direction were seen in HDPE-A and had mean size of 24.3 nm. The crystals of HDPE-W and HDPE-WI were smaller, with dimensions of 20.6 nm and 19.7 nm, respectively.

Results of the tensile drawing for compression-molded HDPE samples are presented in Fig. 1a. Examined samples had thickness of 1 mm and were prepared by different cooling procedures: slow in the air, faster in the water and very fast by immersing in a mixture of water with ice. The test was stopped at the engineering strain of 75%, before the break of material. The yielding with formation of a neck was observed for all samples. Fig. 1a shows that the yield stress strongly depended on crystallization conditions and it was 26 MPa for HDPE-A, 21 MPa for HDPE-W and only 19 MPa for HDPE-WI. The yield strain increased from 13% for HDPE-A, through 18% for HDPE-W to 19% for HDPE-WI.

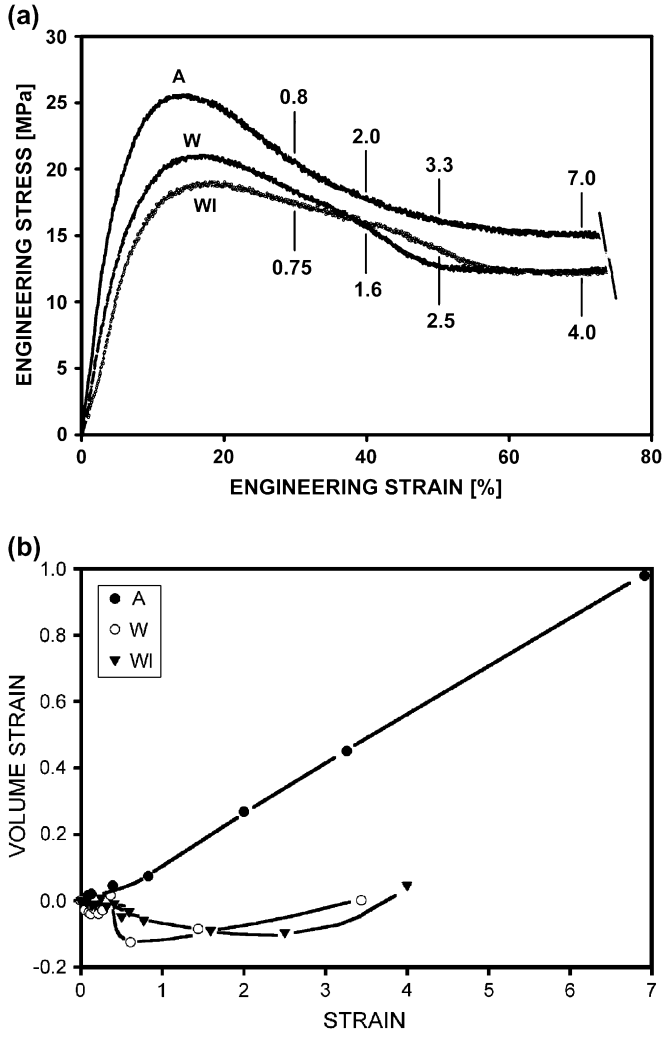

Fig. 1. (a) Engineering stress–strain curves for compression-molded HDPE samples deformed to 75% of engineering strain. Different cooling procedures were applied during preparation: A – sample cooled in the air (HDPE-A), W – sample cooled in the water (HDPE-W), WI – sample cooled in the water with ice (HDPE-WI). Numbers near curves indicate strains measured in the most deformed parts of samples. (b) Volume strain of HDPE as a function of strain for different cooling procedures (as above).

Thickness of the samples did not play an important role – for the 4 mm thick HDPE-A sample the yield stress was 25.5 MPa and yield strain 12% (not shown in Fig. 1a) as compared to 26 MPa and 13% for 1 mm thick plate.

An intensive whitening in the neck area was visible in compression-molded samples cooled in the air (HDPE-A). The translucency of HDPE-WI samples, cooled in the water with ice, was not affected by deformation. In the third material, HDPE-W, cooled in the water, the translucency was changed only a little.

Fig. 1b presents dependence of volume strain on strain. The volume of analyzed, the most deformed part of the sample was nearly constant in the case of HDPE-W and HDPE-WI specimens. A small decrease of volume, which is outside the limits of experimental error, observed at strains of 0.5–2.5, may be attributed to the volume compaction of the amorphous phase due to orientation [36,37]. There is a rapid increase of volume strain for the HDPE-A sample when the strain exceeds 0.4. At strain of 7.0 the volume of deformed part is twice of the initial one. Such a large increase of the volume in HDPE-A may be explained by the formation and growth of cavities. This explanation is supported by the results of SAXS studies presented below.

The images of small angle X-ray scattering patterns from compression-molded samples deformed to 75% of engineering strain are shown in Fig. 2. The objects of studies were the most deformed parts of stressed samples, where the strain was 4.5. Some orientation of crystalline elements is visible in the samples of HDPE-WI and HDPE-W (Fig. 2a and b). In the second case a trace of cavitation is seen as two black streaks in the direction perpendicular to the drawing direction. Very intensive scattering from voids was recorded for the HDPE-A specimen (Fig. 2c). The voids in HDPE-A are elongated in the drawing direction, as it is evidenced by the shape of a scattering image.

Comparison of X-ray scattering images with mechanical properties and results presented in Table 1 leads to the conclusion that if the crystallinity is high and crystals are thick, then the higher stress level is reached and the cavitation occurs. On the other hand, if the crystals are thinner and the polymer is less ordered, then the observed macroscopic yielding is controlled by the plastic deformation of crystals and voids are not present. This conclusion is in agreement with our earlier observation of competition between cavitation and crystal plasticity for other polymers [19].

Fig. 3 shows images of X-ray scattering from HDPE-A samples deformed to strains of 0.02, 0.13, 0.3 and 2.1. The strain of 0.02 is a limit of linear elastic response. Voids at this deformation were not visible. Also at the yield, when the strain was equal to 0.13 the cavities were not detected (Fig. 3b). The cross-section area of the sample at yield was equal to 93% of the initial area and determined true stress, 27 MPa, was too low to initiate cavitation with stable voids of a size detectable by our SAXS. The cavitation was seen after yield (Fig. 3c). At a larger strain of 2.1, when the neck was well established, the intensive scattering from voids was observed in the whole neck (Fig. 3d). The measured engineering

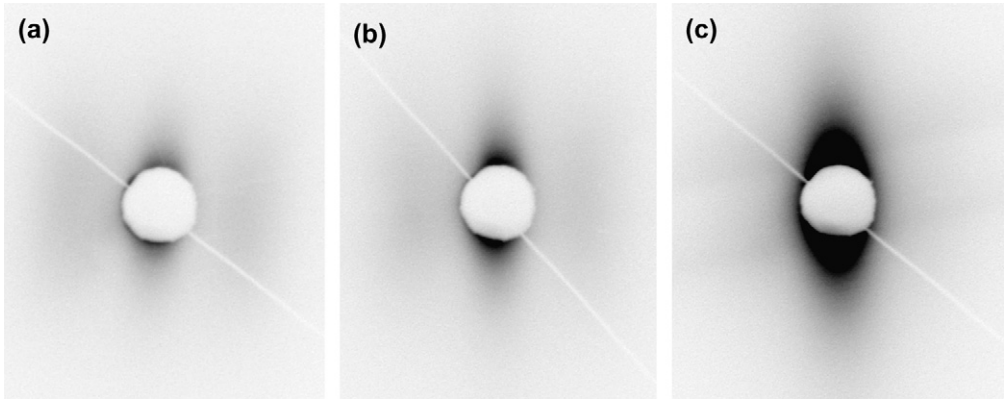

Fig. 2. SAXS images of stressed samples with local strain of 4.5: (a) HDPE-WI, (b) HDPE-W, and (c) HDPE-A. The deformation direction was horizontal.

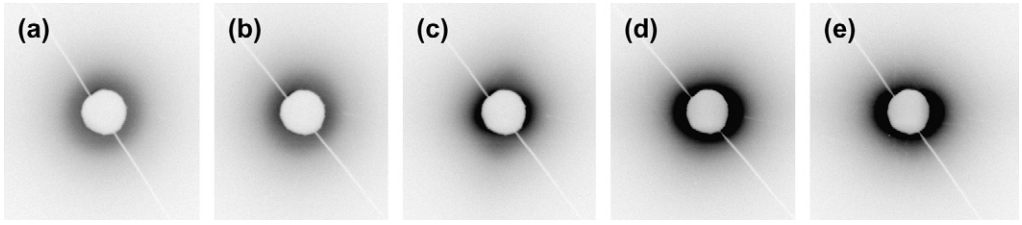

Fig. 3. X-ray scattering from HDPE-A samples deformed at different strains: (a) 0.02, (b) 0.13, (c) 0.3, (d) 2.1, and (e) 2.1 − observation of the same sample as (d) but in the perpendicular direction. The stress state in samples was fixed. The deformation direction was horizontal.

stress was here around 23 MPa, however due to localization of plastic deformation the true stress in mostly deformed part of the sample was 29 MPa. Voids at this deformation were approximately ellipsoidal (which was confirmed by an additional SAXS observation in perpendicular direction, Fig. 3e). The similar scattering phenomena were observed also for 2 mm and 4 mm thick HDPE-A samples.

The scattering patterns seen in Fig. 3c and d were the sources of information about voids' sizes, determined by Yamashita's approach [28]. The radii of gyration, R_g, for voids were between 4 nm and 11 nm when the strain was equal to 0.3 (Fig. 3c). The fraction of largest cavities with $R_g = 9-11$ nm in their total number was 24%. There were 40% of intermediate size cavities ($R_g = 6-8$ nm) and 36% of small voids, with $R_g = 4-5$ nm. All these values of R_g were determined in the direction parallel to deformation. The scattering from voids in the direction perpendicular to elongation was not observed. It means that the sizes of cavities in the second direction were outside the measuring limits. The shape of scattering pattern and above presented values of R_g, which depends on all dimensions of cavities, suggest that the voids had large dimensions (>40 nm) in perpendicular direction and the scattering connected with them is located in the center of photographs, covered by the beam stop. If ellipsoidal shape of cavities is assumed their dimensions can be evaluated from the relation $R_g^2 = (2a^2 + 2b^2)/5$, where $2a$ and $2b$ are the lengths of ellipsoid axes [38]. If we assume that b is the half of amorphous layer thickness, i.e. $b = 3.5$ nm, then the longer axis of largest cavities (with $R_g = 11$ nm) is equal to 48 nm.

When the strain increases to 2.1 the shape of scattering from cavities changes (Fig. 3d and e) to intermediate between those shown in Figs. 3c and 2c. R_g values, measured at this strain in the deformation direction, were between 2 nm and 18 nm. A small (5%) population of large voids was present, with $R_g = 15-18$ nm and also the group of voids (20%) with $R_g = 2-3$ nm.

The measurements of scattering in perpendicular direction gave results of R_g between 4 nm and 25 nm, however, the population of largest cavities, with $R_g = 21-25$ nm, was small (5%) and in the sample dominated cavities with $R_g = 4-10$ nm. Similar results were obtained for the second perpendicular direction, determined from Fig. 3e. Comparison of results for scattering in the direction parallel and perpendicular to deformation suggests that voids at strain of 2.1 were less elongated than those observed for the strain of 0.3. In all scattering images, presented in Fig. 3, small voids, with $R_g < 2$ nm, were not detected.

It is known from the paper [19] that the yield stress of HDPE is significantly lower when measured in a tensile test as compared with that measured in a channel die compression test. It means that the cavitation influences yielding process and suggests that small cavities are formed shortly before yielding. However, the voids were not detected by SAXS for reasons discussed below.

The crystallinity of HDPE-A is 80% and long period for initial material measured by SAXS is 26.4 nm. Calculations show that the thickness of amorphous layer between lamellae is 5.3 nm. The elastic deformation of polymer mainly concentrates in its amorphous phase and only some rotations of crystalline stacks are activated. If we assumed that the deformation of amorphous phase at yield is 25%, not 13% as for whole sample, the thickness of amorphous layer at yield increases

to 7 nm. The same value of 7 nm was obtained from correlation function, determined from X-ray scattering data. The stress at yield, which is 26 MPa, generates negative pressure of around −17 MPa inside the material [19]. This negative pressure is enough to initiate cavitation. Since cavities are very small, there is a problem of their stability. On each void the surface tension is exerted from the beginning of its formation, which tends to close a pore. In order to preserve a void, the action of a negative pressure is required at the level which is reciprocally proportional to the pore radius: $p = -2\gamma_s/r$, where γ_s is the surface tension (35.7 mJ/m^2 [39]) and r is the size of a pore. It follows then that the smallest pores are healed readily, while larger ones can be preserved if the negative pressure is maintained at a sufficiently high level.

The negative pressure value at yield is approximately 2/3 of macroscopic stress, i.e. it is around −17 MPa and stabilize spherical voids with radius of 4.2 nm and more. However, the half of amorphous layer thickness is equal to 3.5 nm, and due to this only smaller, non-stable voids may be formed in this layer. The evidence of such cavitation with healing voids was presented for Nylon 6 by Galeski et al. [40] and explained in [19]. The small voids in HDPE disturb the internal stress state, increasing the concentration of stresses in some places. Non-uniform stress distribution favors the initiation of plastic deformation of lamellae at lower macroscopic stress level.

The engineering stress–strain dependence for tensile deformation of injection-molded HDPE-I is shown in Fig. 4a. The test was stopped at the engineering strain of 75%. HDPE-I had a similar yield stress (26 MPa) as HDPE-A, but a lower yield strain (10%). Respective changes in the volume strain are shown in Fig. 4b. The curve in Fig. 4b represents typical dependence of volume strain on strain. In the region of elastic deformation the measured volume strain was below 0.02 for all tested samples. The increase of volume due to cavitation is seen for strains in the range of 0.3–2.0. Plastic deformation in this range of strains is going through the formation of neck. Careful studies show that the actual shape of neck may change from sample to sample, which gives different values of volume strain for individual samples, dependent on the neck development. When the strain reaches the value of ≈2.0 the neck becomes well developed and the measured volume strains are again similar for all samples.

The maximum volume strain of 0.25 is observed for strain of 2.0 and it stabilizes for large deformations. The region of constant volume strain is in the same range of strains as the plateau of stress in Fig. 4a. Observed dependence is a result of strong localization of deformation in neck. The high strain of 5.0 was measured in HDPE specimen when the engineering strain was only 75%.

The development of voids in injection-molded HDPE-I was followed by SAXS in such a way that the gauge of a stressed sample was fixed in a special frame when the stress reached a requested level. The sample with fixed length was then exposed in the SAXS camera. For each stress marked on Fig. 5 a fresh sample was prepared and stretched.

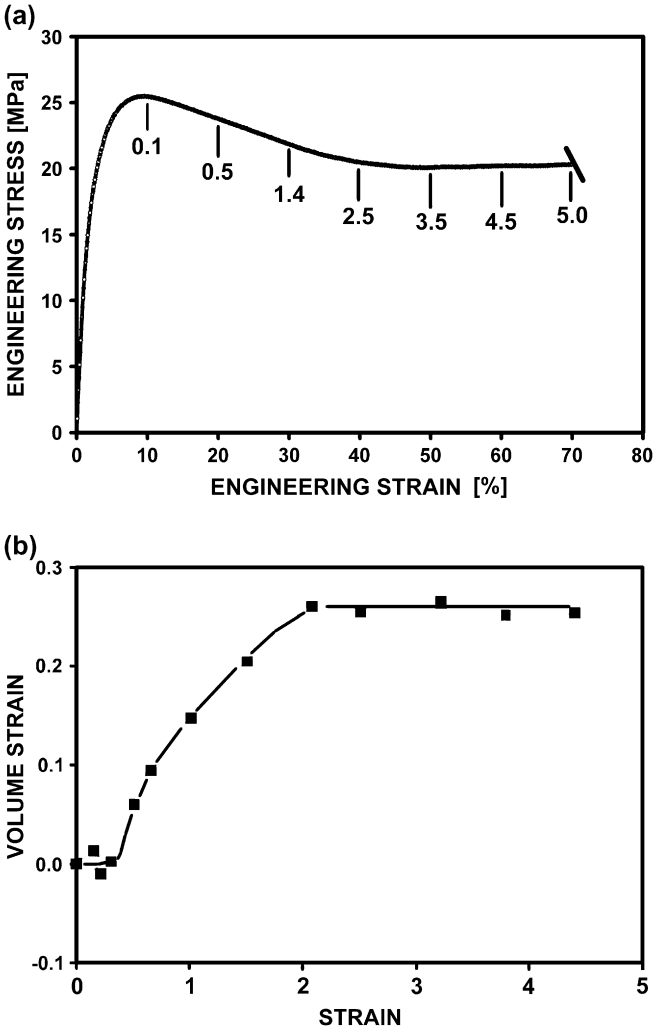

Fig. 4. (a) Stress–strain curve for injection-molded HDPE-I. Numbers below the curve indicate strains. (b) Volume strain of HDPE-I as a function of strain.

Fig. 5 shows the evolution of X-ray scattering pattern with the increase of applied stress to the injection-molded HDPE-I. An unexpected intensive voiding is observed at the very early stage of deformation, of only 0.15%, i.e. at the stress of 2 MPa. The two-point SAXS pattern suggests that the voids are already not spherical. For samples with further increased stress the two-point pattern does not change its shape and only the intensity of scattering increases further. Intensity of scattering at the stress of 25 MPa is around 50% higher than the intensity at the stress of 2 MPa. The analysis of those scattering patterns by Yamashita approach [28] shows that the radii of gyration, R_g, for voids are between 0.5 nm and 15.5 nm. The values of R_g were determined in the direction parallel to deformation. The scattering from voids in the direction perpendicular to elongation was not observed.

If we again assume that the voids in HDPE-I are elongated and one of their dimensions, b, is the half of amorphous layer thickness, i.e. 3.5 nm, then the elongation of largest cavities (with $R_g = 15$ nm) calculated from the relation $R_g^2 = (a^2 + 2b^2)/5$ is equal to 66 nm.

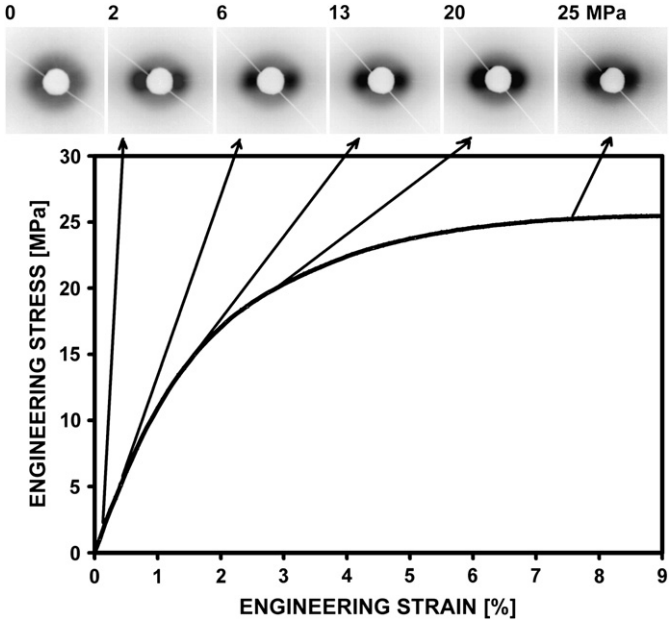

Fig. 5. The evolution of SAXS scattering pattern with the increase of stress applied to the HDPE-I. Deformation direction was horizontal.

The careful scrutiny of SAXS patterns in Fig. 5 does not reveal any evidence of internal structure of voids, such as ligaments in crazes. The increase of applied stress from 2 MPa to 25 MPa does not really significantly influence the thickness of cavities. Values of R_g are in the range of 1.1–15.4 nm, when the stress is 25 MPa. However, in the more deformed samples an increase of the number of large voids is observed, those with $R_g = 15.4$ nm. The number fraction occupied by large voids in the sample deformed to yield point reaches 90% while it is only 65% for the sample stressed to 2 MPa. In both cases the approximation of ellipsoidal shape ($a/b = 10$) for the large and small cavities was applied in calculations.

Such large differences in cavitation behavior between compression-molded and injection-molded samples must have the reason in morphology of injection moldings. In order to localize the cavities in injection-molded bars, skin layers of different thickness were removed by machining 4 mm thick undeformed HDPE-I samples. The samples after thinning were deformed in tensile drawing to reach the stress level of 13 MPa (around 1.2% of strain) and then SAXS patterns were registered while the samples were still in the stressed state. Results of X-ray scattering from the stressed specimens are presented in Fig. 6a. Removal of 75 μm thick layers from each side of the sample did not change markedly the intensity of scattering from voids. After thinning by 0.45 mm equally from both sides to $d = 3.10$ mm, the scattering from voids became much less intensive. When the sample thickness was only 2.2 mm (thinning both sides by 0.9 mm), cavities were not detected.

Fig. 6b shows the image of small angle X-ray scattering when a 1.7 mm thick layer was removed only from one side of the injected sample before drawing. An intensive signal from voids is visible. It confirms that the scattering observed at low deformations for injected samples is a result of cavitation in 0.4–0.5 mm thick surface layers.

Although the cavities are located in the amorphous layer it is obvious that the conditions of cavitation depends on the morphology of whole sample. The results of differential scanning calorimetry and X-ray diffraction for skin and core parts of HDPE-I and HDPE-A are collected in Table 2. The lamellae in HDPE-I are thinner and total crystallinity is lower than in HDPE-A. Also the melting temperature of crystalline phase is lower in HDPE-I than in HDPE-A in core and in skin, respectively. The crystals in HDPE-I skin had thickness close to the crystals of non-cavitating HDPE-WI (see Table 1 for comparison). Measured changes in crystallinity and lamellae thickness do not explain the observed early cavitation in HDPE-I skin.

Examples of typical morphologies of skin and core of injection-molded samples are illustrated in Fig. 7. The polymer flow direction during injection is vertical. On both micrographs lamellar structure is clearly visible. Fig. 7a shows the central part of injection-molded sample, while the micrograph in Fig. 7b represents the skin area of the sample at the distance of 50–60 μm from its surface. Lamellae in the volume of the sample (Fig. 7a) are not preferentially oriented. However, in skin layer, seen in Fig. 7b, an orientation of lamellae perpendicular to the flow direction is visible. The SEM observations reveal that lamellae preferred orientation declines at the distance of 150–200 μm from the surface.

SAXS measurements performed for elastic range of deformation showed continuous increase in lamellae long period,

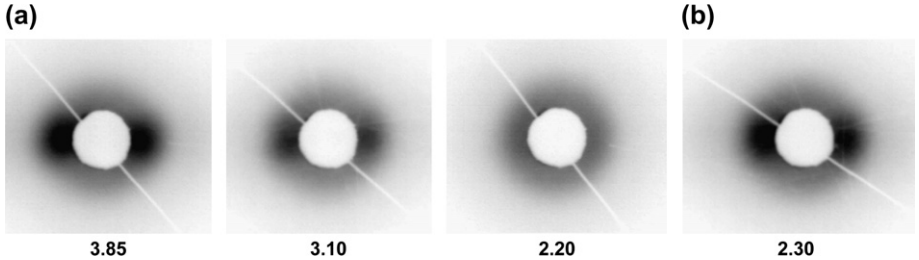

Fig. 6. SAXS patterns from injection-molded HDPE-I samples in which surface layers of different thickness were removed before the tensile test. The deformation direction was horizontal and the test was stopped at the stress level of 13 MPa. (a) Scattering from samples with skin layers removed from both sides. Numbers below photographs indicate local thickness in millimeter. (b) Image of X-ray scattering from the sample with a layer removed from one side only. Thickness of the examined place was 2.3 mm.

Table 2
DSC, WAXS and SAXS results for 4 mm thick HDPE-I and HDPE-A samples

Sample	Position inside the sample	Crystallinity degree by DSC [%]	Crystallinity degree by WAXS [%]	Melting temperature [°C]	Crystalline stem length by DSC [nm]	Lamellae thickness by DSC [nm]	Lamellae thickness by SAXS [nm]
HDPE-I	Skin	68	70	132.5	21.6	17.7	14.5
	Core	73	71	134.3	25.6	21.0	18.7
HDPE-A	Skin	79	74	135.1	27.0	22.1	22.5
	Core	78	72.5	136.7	28.5	23.3	22.9

both in the skin and in the volume of HDPE-I, however, to a different level. The long period in the skin increased from 21.3 nm to 24.0 nm at yield, i.e. 11%, which agrees with 10% of macro scale deformation. If the lamellae are arranged as in Fig. 7b, crystallinity is 68% and all deformation happens in the amorphous phase it means that average thickness of amorphous layer increases from 6.8 nm to 9.5 nm, i.e. around 40%.

The long period measured in deformation direction for volume part of HDPE-I sample increases from 25.6 nm for non-deformed specimen to 26.8 nm if strained to yield. It is only 5% increase, less than 10% of macro deformation. Probably the rest of deformation is a result of interlamellar shear and lamellar stack rotation. The deformation of amorphous phase between lamellae, calculated as above, is here much smaller, only 20%.

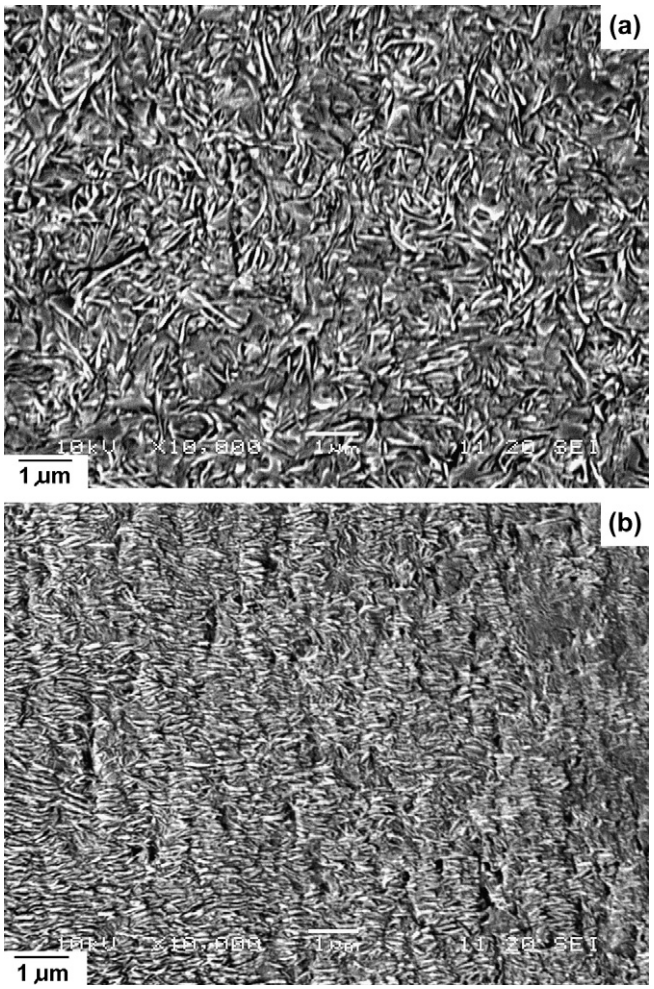

Fig. 7. SEM micrographs of etched, non-deformed HDPE-I samples: (a) core and (b) skin. The center of the area in (b) is at the distance of 50–60 μm on the left from the sample surface.

The SAXS experiment (Figs. 5 and 6) showed that the cavitation is visible only in the skin layer of the HDPE-I sample drawn up to yielding. The evolution of the shape of cavities after yielding may be deduced from SAXS patterns presented in Fig. 8. Fig. 8 represents scattering from 300 μm thick slices of the skin layer of HDPE-I samples deformed to the increasing strain. The slices were cut from surface of sample, deformed previously to the engineering strain of 75%. Each slice had different strains, representing subsequent steps of plastic deformation. The range of strain was from 0 (initial) to 4.5.

There is a rapid change of scattering pattern shortly after the yield. The calculations of occupation volumes by cavities suggest that some new cavities were formed, because at the strain of 0.5 the contribution of largest cavities is only 33% of total number of cavities, whereas at yield they occupied 90%. Again Yamashita's [28] approach was used here for calculations. The SAXS signal for strains from 0.5 to 1.8 has the shape of two arcs around central beam stop. A slow increase in total scattering in this strain range and small change of shape up to strain of 1.8 may be interpreted as a continuous enlargement of existing cavities without changes of their orientation. Probably also the number of cavities increases, because in this deformation range the volume strain increases by 25% (see Fig. 4b). The second rapid change of SAXS pattern was observed for strain of 3.4. Such change of the SAXS pattern was previously described by Butler et al. [6] and explained as the change in the shape of cavities from perpendicular elongation to deformation to elongation in the drawing direction. When the sample is deformed more the gradual voids enlargement occurs and the intense X-ray scattering from large voids is at very low angles, difficult to detect by SAXS.

Cavities in the core of injected HDPE are formed later than those in the skin layer.

Fig. 9 presents SAXS images from the core of deformed injected bar. Here, after the deformation of the sample to engineering strain of 75%, the 0.5 mm thick skin layers were removed from both sides of the bar and the core of sample was studied. Similarly as in Fig. 8, the fragments of the sample with the strain from 0 to 4.5 were analyzed. Undeformed polymer shows still some small, perpendicular orientation of lamellae, as it is seen from the SAXS pattern. The orientation is lost when the sample is deformed to yield. This is the result of reorientation of lamellae due to mechanisms such as

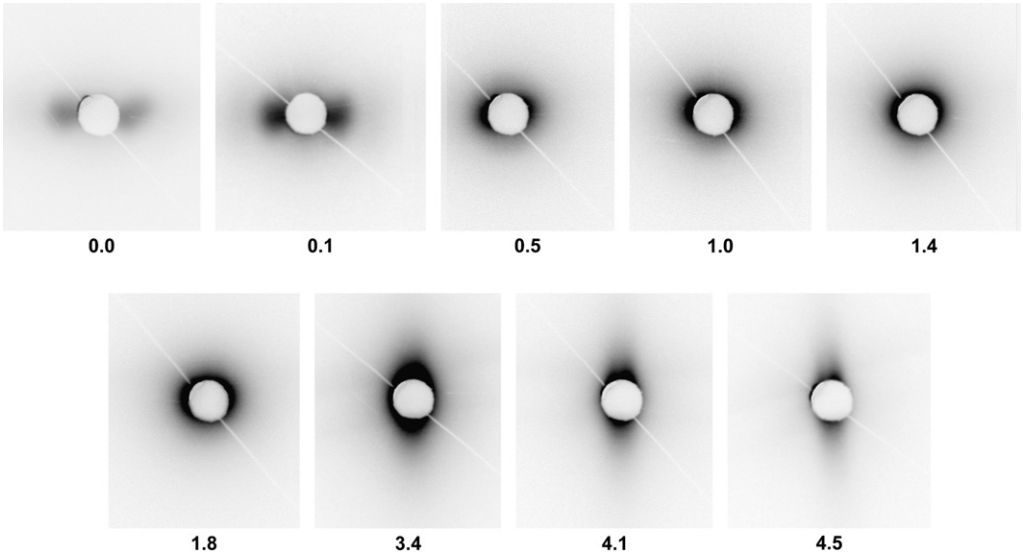

Fig. 8. SAXS scattering from 300 μm thick skin layer of deformed HDPE-I sample. Deformation direction was horizontal. The numbers represent strain.

interlamellar shear or lamellar stack rotation [6]. Some traces of the scattering from voids were detected after yielding at the strain of 0.3–0.4. These cavities were formed at the stress level of 29–30 MPa. The scattering from those voids is rather weak, concentrated close to the beam stop. It has a shape of arc, similarly to the scattering from voids in the skin, indicating perpendicular orientation of voids with respect to the drawing direction. The scattering gradually increases with deformation. At the strain of 1.8 the beginning of voids' reorientation is visible. It occurred at a little lower strain than reorientation of voids in the skin. The reoriented cavities are elongated now in the drawing direction. The elongated streak, observed at strain of 4.1 suggests thinning of reoriented voids. The small angle X-ray scattering for a sample deformed to strain of 4.5 is less intensive and more concentrated near center. It agrees with previous observations [19] that at high strains scattering disappears, due to enlargement of voids beyond the SAXS detection range.

The early cavitation in skin and delayed cavitation in core should be visible macroscopically as the increase in volume strain. The detailed analysis of change of the volume strain, separately for the core and the skin of HDPE-I sample, is presented in Fig. 10. Fig. 10a shows the results for core of HDPE-I based on the measurements of three dimensions of sample during the mechanical test. A 300 μm thick skin layer was removed from each side of the samples for this test. Fig. 10b presents similar data for the skin, however, the data were collected from another experiment for which the skin–core–skin structure was exposed by removing a thin slice (300 μm) from one side of the analyzed sample. In this case particular

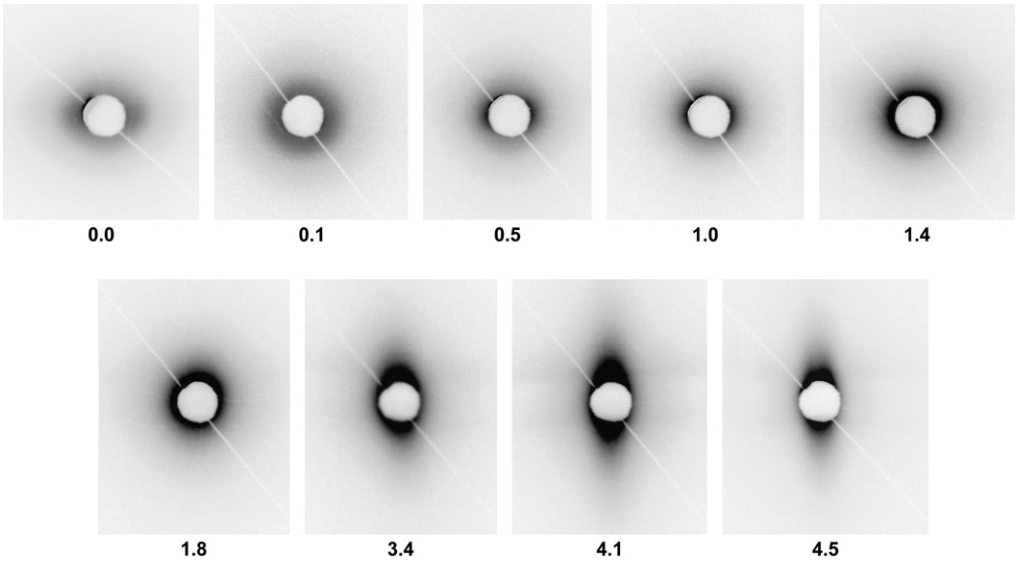

Fig. 9. SAXS patterns obtained from different places in core of HDPE-I sample deformed to 75% of engineering strain. Deformation direction was horizontal. The numbers represent strain.

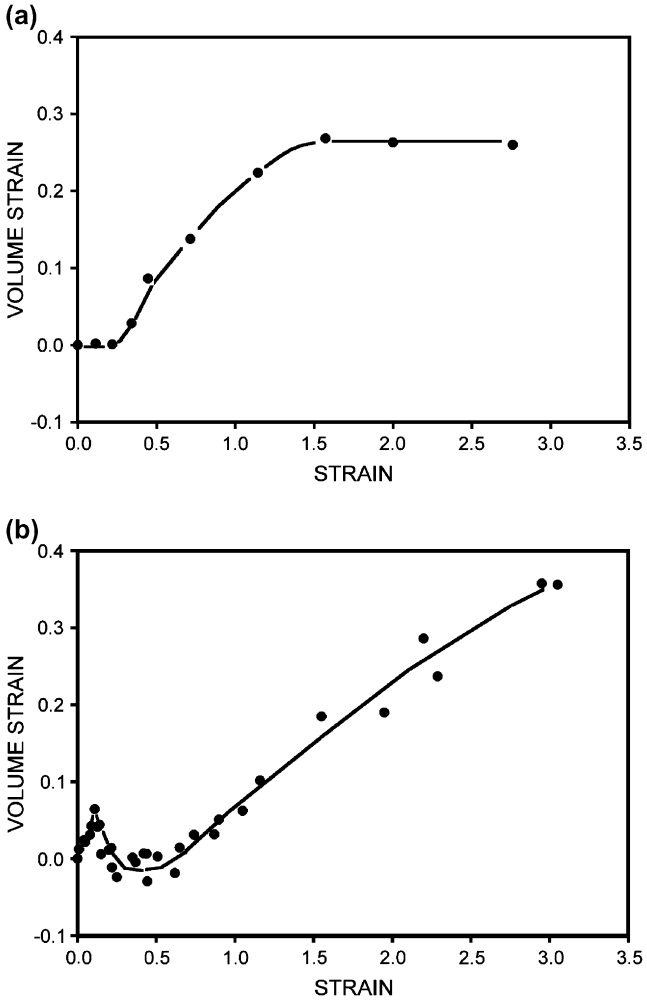

Fig. 10. Volume strain of HDPE-I sample as a function of strain: (a) core and (b) skin.

attention was paid to the accurate measurements of thickness, necessary for the precise determination of volume strain. The distances between the measuring marks were here 0.3 mm.

The volume strain was zero for the core of HDPE-I sample deformed to the yield point. When the strain was in the range of 0.3–1.6 the volume strain rapidly changed and finally there was 28% increase in the volume. This is in good agreement with observations of voids formation presented in Fig. 9.

The volume strains for skin and core changes differently when the deformation is small, before yield strain as it is seen in Fig. 10b. There is an increase of volume strain in skin observed at the very beginning of deformation. The maximum of 0.06 is reached when the strain is around 0.1.

According to the discussion by Quatravaux et al. [36] the volume strain for small deformation includes contributions from elastic deformation and from cavitation. The elastic part $(\Delta V/V_0)_{el}$ can be calculated from relationship $(\Delta V/V_0)_{el} = (1-2\nu)\sigma/E$, where ν and E are Poisson's ratio and Young's modulus, respectively. If for the studied HDPE the values are $\nu = 0.46$, $E = 1050$ MPa [19] and $\sigma = 25$ MPa then $(\Delta V/V_0)_{el} = 0.002$. It means that the volume strain due to elastic response of the material is very small as compared to the entire increase of the volume strain in the skin. The most part of the volume strain in the skin is the result of early cavitation.

Fig. 10b shows that after the yield point the volume strain in the skin decreases approximately to its initial value. SAXS diffractograms presented in Fig. 8 suggest that this decrease is a result of rearrangement of lamellae orientation, accompanied by changing of voids' shape. When the strain is larger than 0.5 again the increase of volume strain is observed. This increase is due to the formation of new cavities, which was also seen in SAXS studies as the change of scattering intensity and an increase of relative content of small voids. The shape of curve representing volume strain in skin is at this range of deformation similar to that for core of HDPE-I. The values of volume strain in skin, determined for strains around 2.0, are very close to those observed for core. However, the maximum volume strain of 0.36 is seen for larger strains than in the case of core. The volume strain of highly deformed skin layer depends also on surface cavitation and this is probably the reason of differences between curves representing skin and core, observed for large deformations.

The cavitation and growth of voids occur in the amorphous layers, but in the neighborhood of crystalline elements. Both phases – crystalline and amorphous – are interconnected by macromolecules and undergo deformation together although in a different way, so the processes in crystalline phase should be studied parallel, as strictly connected with cavitation and deformation of amorphous phase. Some information about the deformation and rearrangement of crystalline elements during plastic deformation can be obtained from wide-angle X-ray scattering. Here the same slices of HDPE-I material were used as previously tested by SAXS (data in Figs. 8 and 9). The results of WAXS studies are presented in Fig. 11 for the skin and in Fig. 12 for the core of injection-molded samples. The direction of stretching in Figs. 11 and 12 is horizontal.

The two circles, which show up in the WAXS patterns, are associated with a scattering of the 200 (outer circle) and 110 (inner circle) lattice planes. Fig. 11 for strain of 0.0 confirms the SEM observations of strong lamellae orientation in the skin of non-deformed HDPE-I sample. This orientation is preserved during the elastic deformation when the strain reaches 0.1. However, after yielding four maxima are formed on the (110) ring and the equatorial maximum of (200) reflection decreases. The four-point pattern of (110) reflection is usually produced by (100) chain slip of PE crystals [14] and it is associated with tilting and begining of fragmentation of lamellae [6,41], initiated by the presence of voids, generating non-uniform stress field.

When the strain is 1.8 a weak ring from monoclinic phase, inner to (110) ring, is visible for the first time. The monoclinic phase is a result of martensitic transition from the orthorhombic phase. This transition is usually observed after relaxation of stress. All pictures in Fig. 11 were collected after the mechanical test and relaxation of stress. When the macroscopic stress level reaches plateau and strain is around 1.9–3.3 a fibrillar texture begins to form. This is visible in WAXS

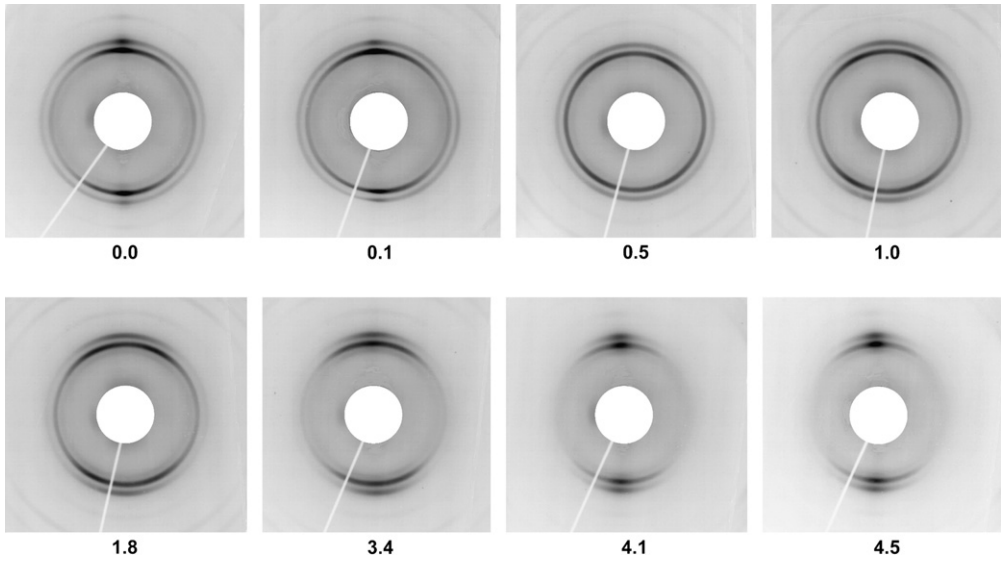

Fig. 11. Wide-angle X-ray scattering from the skin layer of HDPE-I. Differently deformed places were analyzed. Stretching direction was horizontal. Numbers represent strain.

patterns as arcs, concentrating near the equator for all (*hk*0) reflections.

Fig. 12 presents WAXS scattering from differently deformed places in the core of tested sample. All measurements were done after mechanical test and removing skin layers. The weak orientation of lamellae in the core is observed during elastic part of deformation. This is in agreement with SAXS observations (see Fig. 9). After the yield four-point image of (110) ring was formed. Also the decrease of intensity of scattering from (200) plane on meridian and increase of it on equator was observed. The development of broad (200) reflection on equator and four-point pattern for (110) reflection at oblique angle are attributed by Strobl [41] in the presence of intralamellar slips. These changes in WAXS patterns are at the same deformation when first time cavitation in volume was detected by SAXS. The four points pattern transition into two arcs is seen for strain of 1.8. The concentration of (200) reflection near the equator is also observed for this strain ratio. A first time transition of orthorhombic to monoclinic phase is registered. The change of scattering pattern means beginning of transition from lamellar to fibrillar structure. It coincidents with changing of voids orientation determined by SAXS. It should be noticed that connection of cavities' reorientation with the beginning of fibrillization was previously observed for skin, although in the second case the effect was registered at different strain ratios.

The WAXS diffractograms for large strains show gradual transition from lamellar to fibrillar structure. It is accompanied

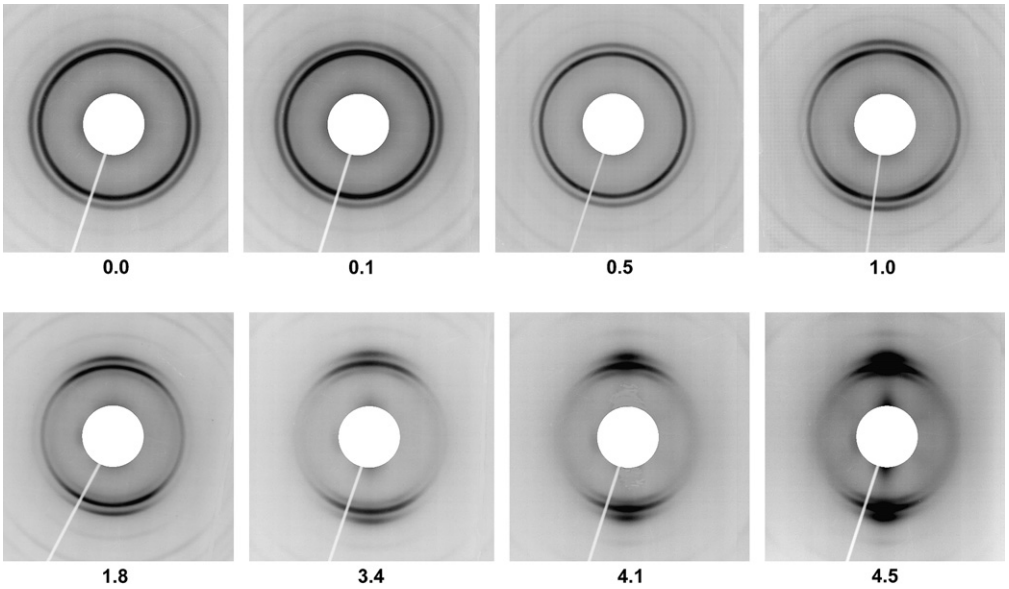

Fig. 12. Wide-angle X-ray scattering from the core of HDPE-I. Differently deformed places were analyzed. Stretching direction was horizontal. Numbers represent strains.

by elongation of cavities in deformation direction, which is seen as equatorial streak (see Fig. 9, strain 4.1).

4. Conclusions

The cavitation process in polyethylene depends strongly on the morphology of studied polymer. Cavitation was observed in those HDPE samples which were cooled more slowly (e.g., HDPE-A and HDPE-I), in which larger and more perfect crystals grew. It is because the crystalline phase tolerates higher stress than the amorphous phase can withstand without voiding. The presence of voids was detected immediately beyond yielding, when the stress level was around 29–30 MPa. Those voids change the stress distribution in polymer, which initiate slips in crystals and contribute to lamellae fragmentation at lower macroscopic stress than was previously measured for the same polymer tested in compression (see [19]). The stable cavities, formed beyond the yield point, are initially located in a small volume of most deformed part of a sample. The volume of voiding increases with deformation.

The cavitation was not observed in polyethylene samples that crystallized fast, by cooling molten material in iced water. In this case, PE crystals were thin and not well developed, and a preferred way of plastic deformation was lamellae sliding and crystallographic slips initiated at yield.

At some conditions the cavitation can occur at a very low strain. An example is the voiding in the skin of injection-molded HDPE sample, where cavitation is observed at 0.15% of strain and 2 MPa of macroscopic stress only. SEM observations show that there is a preferred orientation of lamellae in the skin, perpendicular to the injection direction, resulting from shear and cooling in a mold. The amorphous phase in skin is located between long lamellae and has a shape of elongated layers aligned perpendicular to the injection direction. When the strain within elastic range is applied to such oriented two-phase material the reorientation of crystallites is not present. At these conditions the entire macroscopic deformation is realized in the amorphous phase. Simple calculations, based on crystallinity degree, show that the local strain in this part of HDPE-I may be four times larger than the strain applied in macro scale. Large volume strain initiates cavitation.

Voids change their shape and size during deformation. In the injection-molded HDPE, cavities in the skin layer are initially elongated perpendicular to the drawing direction. Their radii of gyration are in the range of 1–15 nm, preserved up to yielding. Beyond the yield some new small cavities are generated together with the evolution of older voids. When the strain is in the range of 1.9–3.3 the cavities change shape to elongated in the stretching direction. The reshaping is accompanied by the transition from lamellae to fibrillar texture of a sample. Cavities in the skin grow with deformation. Such early cavitation in the skin layer in injection-molded articles makes them vulnerable even to delicate bending, twisting or tensile loading.

The cavities in the core of the injected sample appear later than voids in the skin. They are detected by SAXS when the plastic deformation of crystals is initiated. Also in the core the voids are initially elongated perpendicular to the drawing direction. The change of shape is observed at strain of 1.8, when the beginning of transition from lamellar to fibrillar texture is first seen. It is a moment earlier than was observed for skin. The voids in core of highly deformed HDPE-I sample are elongated in the deformation direction. Similarly as in the skin the cavities grow with increase of deformation level.

A comparison of mechanical and SAXS results shows that the cavities formed in the core of a sample are the major factor influencing the initiation of macroscopic plastic deformation. Beyond yielding the cavities in the core and skin evolve similarly, reacting to the changes in sample morphology.

Acknowledgment

The author would like to thank Prof. A. Galeski for valuable discussion.

References

[1] Duffo P, Monasse B, Haudin JM, G'Sell C, Dahoun A. J Mater Sci 1995; 30(3):701–11.
[2] Li JX, Cheung WL. Polymer 1999;40(8):2089–102.
[3] Butler MF, Donald AM, Ryan AJ. Polymer 1997;38(22):5521–38.
[4] Castagnet S, Girault S, Gacougnolle JL, Dang P. Polymer 2000;41(21): 7523–30.
[5] Nathani H, Dasari A, Misra RDK. Acta Mater 2004;52(11):3217–27.
[6] Butler MF, Donald AM, Ryan AJ. Polymer 1998;39(1):39–52.
[7] Gencur SJ, Rimnac CM, Kurtz SM. Biomaterials 2003;24(22):3947–54.
[8] Galeski A. Prog Polym Sci 2003;28(12):1643–99.
[9] Crist B. Polym Commun 1989;30(3):69–71.
[10] Young RJ. Mater Forum 1988;11:210–6.
[11] Lin L, Argon AS. J Mater Sci 1994;29(2):294–323.
[12] Bartczak Z, Galeski A. Polymer 1999;40(13):3677–84.
[13] Haudin JM. Plastic deformation of semi-crystalline polymers. In: Escaig B, G'Sell C, editors. Plastic deformation of amorphous and semi-crystalline materials. Paris: Les Editions de Physique; 1982. p. 291.
[14] Galeski A, Bartczak Z, Argon AS, Cohen RE. Macromolecules 1992; 25(21):5705–18.
[15] Argon AS, Cohen RE. Polymer 2003;44(19):6013–32.
[16] Oleinik EF. Polym Sci Ser C 2003;45:17–117.
[17] Lin L, Argon AS. Macromolecules 1992;25(15):4011–24.
[18] Shinozaki D, Groves GW. J Mater Sci 1973;8(1):71–8.
[19] Pawlak A, Galeski A. Macromolecules 2005;38(23):9688–97.
[20] Piorkowska E, Galeski A. J Polym Sci Part B Polym Phys 1993;31(10): 1285–91.
[21] Brennen CE. Cavitation and bubble dynamics. Oxford: Oxford University Press; 1995. p. 8.
[22] G'Sell C, Hiver JM, Dahoun A. Int J Solids Struct 2002;39(13):3857–72.
[23] Addiego F, Dahoun A, G'Sell C, Hiver JM. Polymer 2006;47(12): 4387–99.
[24] Lazzeri A, Thio YS, Cohen RE. J Appl Polym Sci 2004;91(2):925–35.
[25] Bucknall CB. Toughened plastics. London: Applied Science; 1977.
[26] Grubb DT, Prassad K, Adams W. Polymer 1991;32(7):1167–72.
[27] Smole MS, Gregor-Svetec D. Acta Chim Slov 2002;49(4):773–82.
[28] Yamashita T, Nabeshima Y. Polymer 2000;41(16):6067–79.
[29] Wu J. Polymer 2003;44(26):8033–40.
[30] Hoffman JD. Polymer 1982;23(5):656–70.
[31] Psarski M, Piorkowska E, Galeski A. Macromolecules 2000;33(3): 916–32.
[32] Patel D, Bassett DC. Polymer 2002;43(13):3795–802.
[33] Alexander LE. X-ray diffraction methods in polymer sciences. New York: Wiley-Interscience; 1970. p. 335.
[34] Olley RH, Basset DC. Polymer 1982;23(12):1707–10.

[35] Zhou H, Wilkes GL. Polymer 1997;38(23):5735–47.
[36] Quatravaux T, Elkoun S, G'Sell C, Cangemi L, Meimon Y. J Polym Sci Part B Polym Phys 2002;40(22):2516–22.
[37] Cangemi L, Elkoun S, D'Sell C, Meimon Y. J Appl Polym Sci 2004; 91(3):1784–91.
[38] Janosi A. Z Phys B Condens Matter 1986;63(3):375–81.
[39] Wu S. Polymer interface and adhesion. New York: Marcel Dekker; 1982. p. 88.
[40] Galeski A, Argon AS, Cohen RE. Macromolecules 1988;21(9): 2761–70.
[41] Hiss R, Hobeika S, Lynn C, Strobl G. Macromolecules 1999;32(13): 4390–403.